

# Interaction of human leukocyte elastase with a *N*-aryl azetidinone suicide substrate: Conformational analyses based on the mechanism of action of serine proteinases

I. Vergely,\* P. Laugâa,† and M. Reboud-Ravaux\*

\*Laboratoire d'Enzymologie Moléculaire et Fonctionnelle, Département de Biologie Supramoléculaire et Cellulaire, Institut Jacques Monod, Université Paris VII-Tour 43, Paris, France †Laboratoire de Photobiologie Moléculaire, Département Organisation et Expression du Génome, Institut Jacques Monod, Université Paris VII-Tour 43, Paris, France

The three-dimensional interaction of the enzyme-activated (suicide) inhibitor AA 231-1 [N-(2-chloromethyl)-3,3-difluoro-azetidin-2-one] with human leukocyte elastase has been studied using computer graphics and molecular mechanics. Systematic conformational analyses and energy minimizations have been performed for the inhibitor AA 231-1 and its presumed complexes formed during the enzymatic process of inactivation, i.e., the Michaelis complex, the acyl-enzyme, and the inactivated enzyme with the covalently bound inhibitor. The  $\beta$ -lactam ring characteristics of modeled AA 231-1 were in agreement with crystallographic data of related structures. Lowest energy conformations were found when the angle between the planes of the  $\beta$ -lactam ring and that of its phenyl substituent was about  $-60$  or  $60^\circ$ . To study the interaction with the enzyme, the enzyme-inhibitor complexes were constructed by docking the inhibitor in the active site using enzyme coordinates from an X-ray crystallographic structure. The whole enzyme structure was used for conformational analyses and energy mechanics. Favorable conformations for the Michaelis complex have been obtained in which the carbonyl oxygen of the inhibitor was located in the oxyanion hole and the hydroxyl of Ser195 was in position to interact with the  $\beta$ -lactam carbonyl carbon on the  $\alpha$  face of AA 231-1. Simu-

lations of the approach of the benzylic carbon by the nucleophilic amino acid His40 or His57 through an  $S_N2$  displacement on the halomethyl group of AA 231-1 were performed. The results agreed with the alkylation of the imidazole nitrogen N $\epsilon$ 2 of His57 leading to the inactivated enzyme (bis-adduct form).

**Keywords:** human leukocyte elastase,  $\beta$ -lactam, suicide substrate, molecular modeling, conformational analysis, molecular mechanics, energy minimization

## INTRODUCTION

Molecular modeling techniques are useful in linking together the understanding of the enzyme mechanism and the design of enzyme inhibitors. We report here a method to analyze the interaction of a suicide substrate with human leukocyte elastase (HLE; EC 3.4.21.37), a serine proteinase<sup>1,2</sup> that is a therapeutic target for drug design.<sup>3</sup> This enzyme, whose main normal physiological roles are phagocytosis and tissue remodeling, is also implicated in the pathogenesis of chronic inflammatory diseases (pulmonary emphysema, rheumatoid arthritis, and atherosclerosis) resulting from an imbalance between the enzyme and its major natural inhibitor,  $\alpha$ 1-P1.<sup>4</sup> To supplement the deficient natural inhibitor, a large variety of low molecular weight inhibitors have been designed.<sup>5</sup> Mechanism-based (suicide) inhibitors display the originality of being substrate analogs possessing a latent reactive function unmasked during the catalytic action of the enzyme. Among them, *N*-(2-chloromethylphenyl)-3,3-difluoro-azetidin-2-one or AA

Color Plates for this article are on page 145.

Address reprint requests to: M. Reboud-Ravaux, Laboratoire d'Enzymologie Moléculaire et Fonctionnelle, Département de Biologie Supramoléculaire et Cellulaire, Institut Jacques Monod, Université Paris VII-Tour 43, 2 place Jussieu, 75251 Paris Cedex 05, France.

Received 16 November 1995; accepted 28 May 1996.

231-1<sup>6</sup> was shown to be effective in preventing elastin solubilization, lung elastin fiber degradation, glomerula basement membrane degradation, and intradermal microvascular hemorrhage induced by HLE in guinea pig.<sup>7-9</sup> Whereas numerous crystallographic structure studies of complexes formed between porcine pancreatic elastase (PPE; EC 3.4.21.36) and substrates or inhibitors have been reported, structures of HLE are less documented, mainly because the crystals of this native or complexed enzyme are obtained with difficulty.<sup>10</sup> Only three structures of HLE complexed with peptidic inhibitors have been solved to date.<sup>11-13</sup> Molecular modeling is another approach to structural studies of the interaction of inhibitors with HLE. In an attempt to investigate the interaction of HLE with AA 231-1, we performed an analysis, using computer graphics and molecular mechanics, of the presumed complexes postulated for the inactivation of HLE: the Michaelis complex (Figure 1a), the acyl-enzyme (Figure 1b) and the inactivated enzyme (Figure 1d). We have employed a method based on systematic conformational searches, that identified permissible conformations, combined with energy minimization.

## METHODS

### Workstation and programs

All the computations were performed on a Silicon Graphics station Iris4D-35 and graphics displayed with an Evans and Sutherland PS390 using SYBYL software version 5.5 (Tripos, Inc.<sup>14</sup>). Molecular mechanics were based on the Tripos force field and parameters.<sup>15</sup> Excel 3.0 (Microsoft) was used to run a macro command written to classify conformations into families.

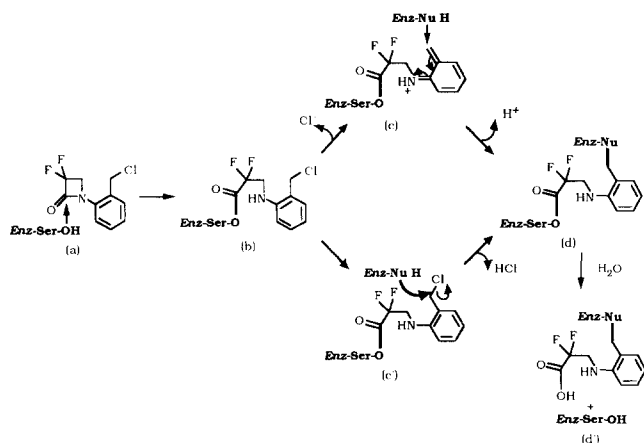


**Figure 1.** Proposed mechanism for the inactivation of HLE by AA 231-1. Initially, a noncovalent complex of Michaelis (a) is formed. The acyl-enzyme complex (b) is constituted after an attack by Ser195.O $\gamma$  on the amide bond of the inhibitor. The process leading to the inactivated enzyme bis-adduct (d) may occur by the reaction of an enzymic nucleophilic group NuH, either with a quinoniminium methylene intermediate generated after departure of the chloride ion (c), or through an S<sub>N</sub>2 mechanism (c'). After hydrolysis of the ester bond, another form of the inactivated enzyme may appear (d').

## Conformational analyses

**Family algorithm** Families were created using the criteria of continuity of rotamer angle values dependent on resolution used: a conformation without a family number is added to family *n* if, for each rotamer, the absolute difference of its angle value with that of at least one conformation of family *n* is equal to zero or resolution value. The latter is the increment value of the systematic conformational analysis. The described algorithm can be used only when a limited number of rotatable bonds and/or conformations are involved.

**Inhibitor** The starting structure of AA 231-1 was built using the X-ray structure of a related *N*-aryl azetidinone, 1-(2-bromophenyl)-azetidin-2-one.<sup>16</sup> After minimization, a conformational analysis was performed. A 360° rotation around the C1'-N1 and C2'-C7' bonds, corresponding to torsional angles RB1 (C4-N1-C1'-C6') and RB2 (C1'-C2'-C7'-Cl), respectively, was allowed with a 1° increment; a scaling factor of 0.9 was applied to atomic van der Waals (vdW) radii (Figure 2). Only conformations without vdW contacts were retained and classified in families using a 1° resolution. The energy of each conformation was calculated.

**Enzyme-inhibitor complexes** Initial coordinates of HLE (devoid of the carbohydrate chains) were generated from the crystallographic structure of HLE complexed with methoxysuccinyl-Ala-Ala-Pro-Ala chloromethyl ketone (Meo-Suc-Ala<sub>2</sub>-Pro-Ala-CH<sub>2</sub>Cl) (PDB file no. 1HNE).<sup>13,17</sup> After removal of all water molecules and of the peptidyl chloromethyl ketone from the active site of HLE, hydrogen atoms and disulfur bridges were added. The new structure (3 321 atoms) was minimized to optimize the X-ray structure until a minimum energy change of 0.05 kcal mol<sup>-1</sup> was reached between two successive iterations. This process did not affect the active site geometry.

The structure of the Michaelis complex leading to the transition state for acylation of Ser195 was constructed according to the accepted hydrolysis mechanism<sup>2</sup> as follows: the inhibitor was docked into the active site in such a way that its carbonyl oxygen laid in the oxyanion hole with convenient hydrogen bond distances of the Gly193 and Ser195 amide hydrogens (2.2 and 1.9 Å, respectively, in the present case). As with native serine proteinases, His57 was

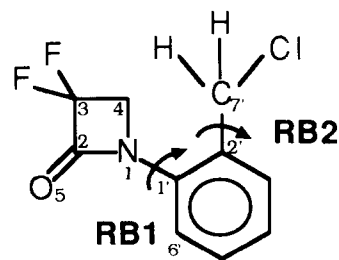


**Figure 2.** Systematic conformational analysis of AA 231-1. Each dihedral angle explores space from 0 to 360°, with 1° increments (vdW scaling factor, 0.9). Arrows show the active rotatable bonds.

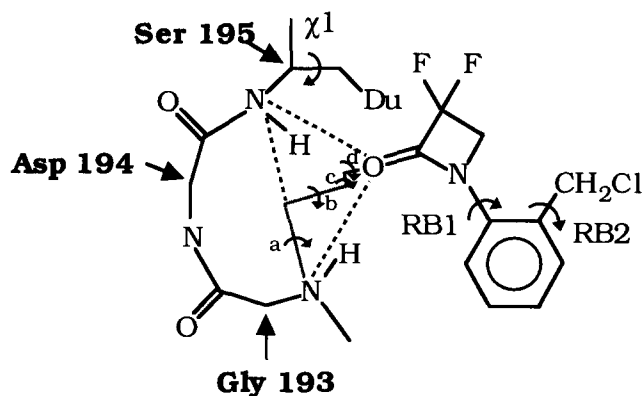


Figure 3. Systematic conformational analysis of the Michaelis complex. The virtual "crank" (gray bonds a–d) maintains the carbonyl oxygen of AA 231-1 in the oxyanion hole; seven rotatable bonds are active (arrows); a 10° increment and vdW factor of 0.85 are applied. Du, Dummy atom.

in the "in" position with His57.Nδ1,<sup>1</sup> the donor, forming a bifurcated hydrogen bond with Asp102.Oδ1 and Asp102.Oδ2, the acceptors.<sup>18</sup> The torsion angles  $\chi_1$  (N–C $\alpha$ –C $\beta$ –C $\gamma$ ) and  $\chi_2$  (C $\alpha$ –C $\beta$ –C $\gamma$ –Nδ1) of the His57 side chain were 66 and –88°, respectively. To allow complete exploration of inhibitor–enzyme interactional space while maintaining the 2.8 and Å donor–acceptor distances of the two hydrogen bonds in the oxyanion hole, we built a crank made of four virtual bonds forming right angles with each other, that connected the nitrogen of Gly193 to the carbonyl oxygen of AA 231-1 (Figure 3). The bond lengths for the successive bonds a, b, c, and d of the crank were 2.15, 1.80, 0.01, and 0.01 Å, respectively. The serine hydroxyl group was replaced by a dummy atom Du to prevent exclusion of conformations with vdW contacts between Ser195.O $\gamma$  and the carbonyl carbon of AA 231-1 (C2). In addition to the two rotatable bonds of AA 231-1 defined above, the crank bonds and Ser195.C $\alpha$ –Ser195.C $\beta$  bond were active. On the whole, with this systematic search, a 360° rotation of seven rotatable bonds was performed with an increment of 10° and atomic vdW radii scaled by a factor of 0.85. This latter value was chosen to allow the attainment of a larger set of conformations. They were then classified into families using a 10° resolution. In each family, the lowest energy conformer was extracted and minimized.

A model of the acyl–enzyme complex (c') was constructed from the above-described minimized structures of the Michaelis complex by opening the  $\beta$ -lactam ring of AA 231-1 and creating a covalent bond between Ser195.O $\gamma$  and AA 231-1.C2 atoms. After minimization, searches were performed with a 360° rotation of nine rotatable bonds using an 20° increment, and a vdW radii scaling factor of 0.9 (Figure 4). As alkylation was assumed to occur by the attack on the AA 231-1.C7' atom by a histidine residue, two possibilities were explored: approach by atom His40.Ne2 or His57.Ne2. In both cases, the AA 231-1.C7' atom was replaced by a dummy atom and a distance range constraint of 1.9–2.7 Å was defined between this atom and the Ne2

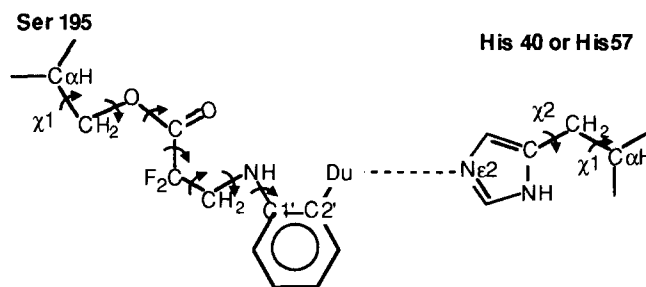


Figure 4. Systematic conformational analysis of the acyl–enzyme (c'). Nine rotatable bonds (arrows) move with a 20° increment (vdW factor, 0.9). A distance range constraint of 1.9 to 2.7 Å is applied between Du and His57.Ne2 atoms.

atom of the histidine. Conformations were then classified in families using a 20° resolution.

Two possible structures could be postulated for the inactivated enzyme: either AA 231-1 formed a covalent bis-adduct with the Ser195 and His57 residues of HLE, or AA 231-1 formed a single covalent adduct with the His57 residue (structures d and d', respectively, in Figure 1). We studied only the former hypothesis, according to which structure d required more steric constraints as it is formed before structure d'. In representative acyl–enzyme conformations, AA 231-1.C7' substituents were removed and a bond was created between this atom and His57.Ne2. A redefining of the imidazole ring atoms and bonds was also needed since His57.Nδ1 was deprotonated. The final structures were then completed by the addition of two hydrogen atoms to AA 231-1.C7' and were minimized.

## RESULTS

### Conformation of AA 231-1

The conformational analysis of the inhibitor led to 22 335 conformations, which were classified in 4 families using a 1° resolution. This distribution is consistent with the two-dimensional representation of torsion angles RB2 against RB1 (Figure 5). In each family, the conformation of lowest energy was extracted and minimized (Table 1, Figure 6). The four resulting conformers (I1–I4) had a similar energy. The relatively high value was due to the constraints of the  $\beta$ -lactam ring. This four-membered ring was nearly planar since the maximum deviation from least-squares plane was less than 0.01 Å. The nitrogen atom was not pyramidal. The conformations were distributed into two classes with respect to the angle between the two cycles of AA 231-1 measured by the value of RB1 angle: around –60° (I3 and I4) or around 60° (I1 and I2).

### Michaelis complex

The conformational analysis of the Michaelis complex (see Figure 3) yielded 10 455 conformers. We then retained only the structures in agreement with the stereoelectronic requirements for the chemical attack of a carbonyl carbon by an oxygen atom,<sup>19</sup> i.e., a range of 1.8–2.6 Å for the distance d1 between the AA 231-1.C2 and Ser195.O $\gamma$  atoms and a range of 80–120° for the angle  $\alpha$  Ser195.O $\gamma$ –AA 231-1.C2–

<sup>1</sup> Examples of atom notation: His57.C $\alpha$  (C $\alpha$  in His57 residue); AA 231-1.C7' (atom of AA 231-1 named C7').

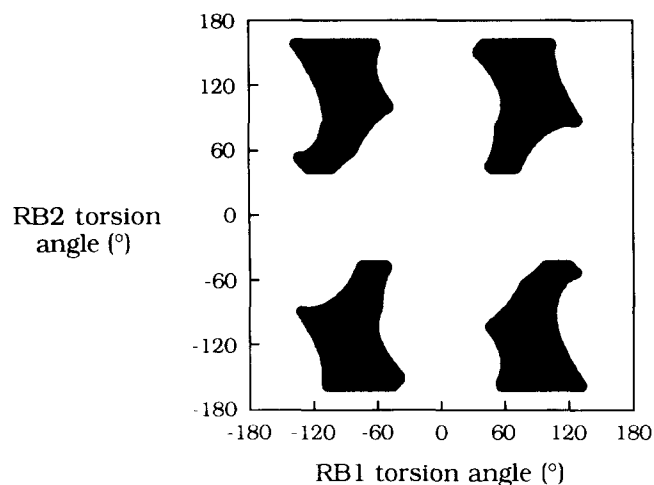


Figure 5. Plot of RB2 against RB1 torsion angles (°) for the conformational analysis of AA 231-1 (see Methods for definition of RB1 and RB2). Black areas correspond to allowed torsional angles.

AA 231-1.O5. This led to 728 conformations distributed in 10 families using a 10° resolution. Ninety-seven percent of these conformations belonged to four major families, which were further studied by extraction of the conformer of lowest energy. After replacing the dummy atom of Ser195 by a hydroxyl group, the four conformers were minimized by imposing the following distance range constraints: 2.7–3.1 Å between Gly193.N and AA 231-1.O5, and between Ser195.N and AA 231-1.O5 (inhibitor oxygen atom situated in the oxyanion hole), 2.0–2.4 Å between Ser195.O $\gamma$  and AA 231-1.C2. Only residues surrounding the barycenter of Gly193.N and Ser195.N within a radius of 15 Å were allowed to move. The results for the four minimized conformers of the Michaelis complex (MC) are summarized in Table 2. The inhibitor adopted two main conformations differing in the angle between the phenyl and the  $\beta$ -lactam rings: RB1 value around  $-157^\circ$  for MC1 and MC2 (group I) and  $134^\circ$  for MC3 and MC4 conformers (group II) (Color Plate 1). The amide bond of the inhibitor was perpendicular to the axis of the  $\beta$ -sheet Ser214-Arg217. The  $\beta$ -lactam cycle occupied the S<sub>1</sub> subsite (Schechter and Berger notation<sup>20</sup>). The fluorine atoms were in close proximity to the Phe192, Ser195, and Val216 residues. The phenyl moiety of AA 231-1 was also close to the imidazole ring of His57 and to the phenyl group of Phe192. An edge-to-face interaction is observed between the phenyl cycles of Phe192 and AA 231-1: distance between the centroids of these two cycles (d2) in the range 5.9–6.4 Å and angle between the two

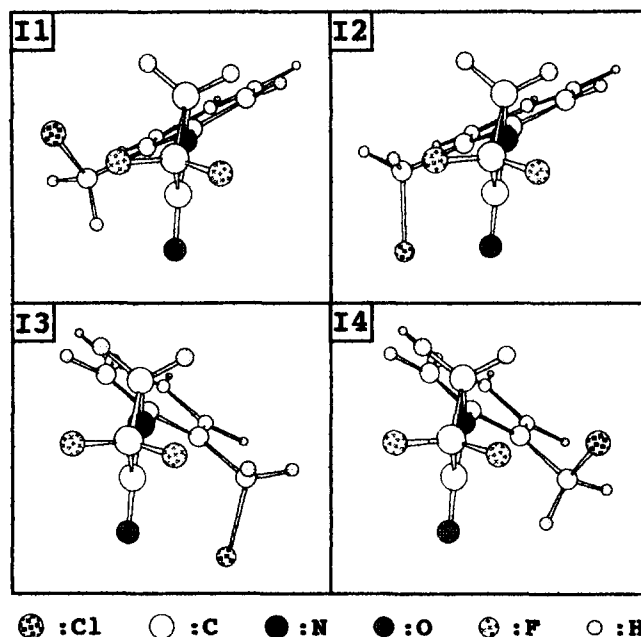


Figure 6. Representative conformers of AA 231-1 (I1–I4). On the basis of RB1 value, two classes of conformers are distinguished: (I1, I2) and (I3, I4). In each class, the chlorine atom occupies two positions: C–Cl bond direction opposite to (I1, I4) or the same as (I2, I3) the direction of the C–O bond.

corresponding planes in the range  $70$ – $77^\circ$  (Table 2). The conformation of the side chain of Ser195 was constrained and characterized by an average  $\chi_1$  angle value of  $-75 \pm 1^\circ$ . The direction of one of the lone pairs of Ser195.O $\gamma$  was perpendicular to the  $\beta$ -lactam ring plane. Average values for distance d1 and angle  $\alpha$  are  $2.5 \pm 0.001$  Å and  $84 \pm 2^\circ$ , respectively. The hydroxyl group of Ser195 was correctly positioned to interact with the inhibitor carbonyl carbon on the  $\alpha$  face of the  $\beta$ -lactam ring (Figure 7). Although the orientation of the  $\beta$ -lactam ring in the active site was roughly the same for all conformers, it should be noticed that in group II, the two hydrogen bonds of the oxyanion hole (HB1 and HB2), implicating the inhibitor oxygen, could be formed, whereas in group I, only formation of HB1 was plausible (Figure 7). Hydrogen bonds between the amino acids of the catalytic triad were still observed. No suitably oriented acceptor in HLE appeared able to create a hydrogen bond with the fluorine atoms of AA 231-1.

### Acyl-enzyme

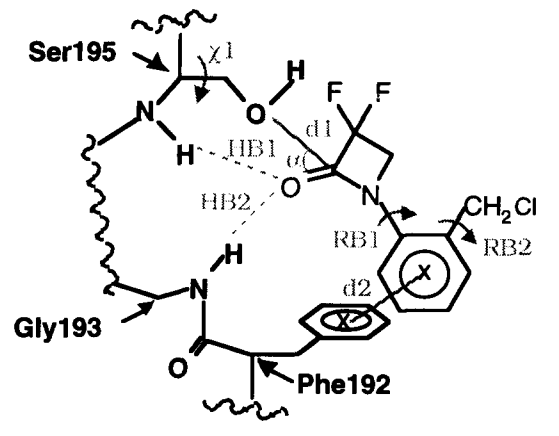
Acyl-enzyme structures were built as described in Methods, starting from the four Michaelis complexes described above. After minimization, a systematic search was performed on two representative structures named acyl-enzyme I and acyl-enzyme II deriving from Michaelis complexes MC1 (group I) and MC4 (group II), respectively (see Figure 4). The two acyl-enzymes were chosen on the basis of the largest r.m.s. deviation determined using a fitting procedure with Ser195 and AA 231-1 atoms. To explore the

Table 1. Representative conformers of AA 231-1<sup>a</sup>

Family	RB1 (°)	RB2 (°)	Energy (kcal mol <sup>-1</sup> )
1	58	50	44.4
2	61	-99	44.5
3	-62	97	44.6
4	-59	-53	44.5

<sup>a</sup>The lowest energy conformer of each family was minimized.

**Table 2. Representative conformers of the Michaelis complex formed between AA 231-1 and HLE<sup>a</sup>**



Family	MC1	MC2	MC3	MC4
RB1 (°)	-158	-157	134	134
RB2 (°)	180	179	-162	-160
χ1 (°)	-75	-77	-74	-75
α (°)	87	88	81	80
d1 (Å)	2.5	2.5	2.5	2.5
HB1	+	+	+	+
HB2	-	-	+	+
Angle between the phenyl cycles of Phe192 and AA 231-1 (°)	77	72	71	70
d2 (Å)	6.1	6.4	5.9	5.9
Energy (kcal mol <sup>-1</sup> )	-241.3	-241.2	-242.6	-242.6

<sup>a</sup>The lowest energy conformer of each family was minimized. The "X's" in the figure represent the centroid of the phenyl rings.

alkylation reaction, conformational searches implicating His40 or His57 were both performed. No possible conformation was obtained with His40. Conversely, the studies with His57 yielded 251 979 and 171 485 conformations for acyl-enzyme I and acyl-enzyme II, respectively. Among all conformations, we retained only those having a correct stereochemistry for the attack by the Ne2 atom of His57 of either the chloromethyl group of AA 231-1 through an S<sub>N</sub>2 mechanism, or the methylene quino-nimine group formed after departure of the chloride ion (Michael reaction). To perform this analysis, we used the following criteria deduced from known stereoelectronic constraints for alkylation reactions of imidazole by a benzylic reagent and from crystallographic data concerning imidazoles substituted at the Ne2 position by a benzylic group<sup>21-23</sup>: (1) a range of 2.0–2.4 Å for the distance between His57.Ne2 and AA 231-1.Du atoms, (2) a range of 70–110° for the angle formed by His57.Ne2-AA 231-1.Du-AA 231-1.C2', (3) the plane of His57 perpendicular to that of the phenyl ring of AA 231-1 with the His57.Ne2 lone pair in the same perpendicular direction. These criteria reduced the number of conformations obtained from acyl-enzyme I and acyl-enzyme II to 1 916 and 1 413, respectively. A high degree of similarity was observed between the two interesting sets of conformations (Table 3). Among the 202 and 197 families created

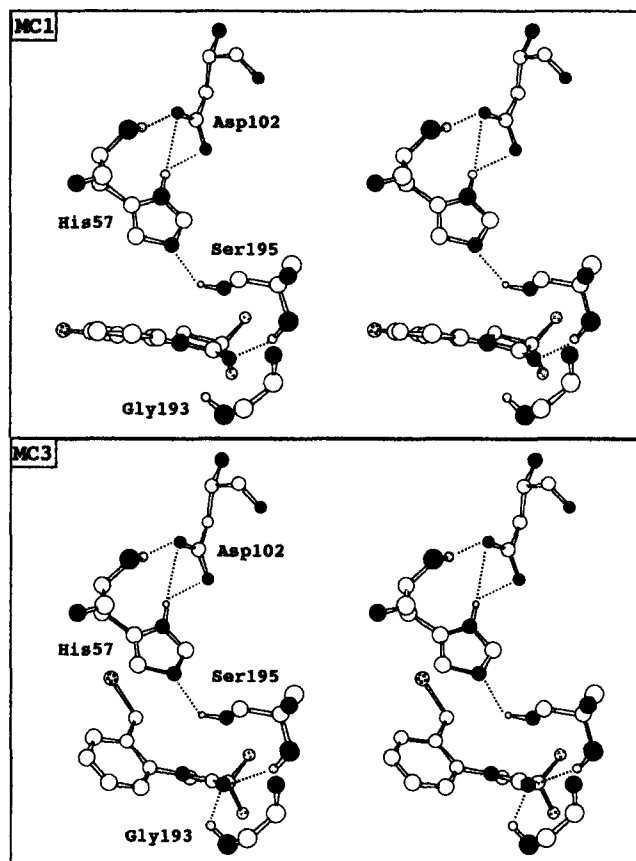


**Figure 7. Stereoview of Michaelis complex conformers MC1 (top) and MC3 (bottom).** Ser195 is positioned for the attack on the carbonyl carbon of AA 231-1 on the α face of the β-lactam ring. The hydrogen bond networks of the catalytic triad (Asp102, His57, and Ser195 residues) and of the oxyanion hole (Gly193 and Ser195 residues) are indicated by dotted lines. In these models, His57 is in the "in" position. Only hydrogen atoms involved in hydrogen bonds are shown. See Figure 6 for symbols.

(20° resolution) for acyl-enzyme I and acyl-enzyme II, respectively, only four large families were found. Each of the four major families of acyl-enzyme I had a link with one of acyl-enzyme II. Grouping the results of both searches allowed us to determine a single representative conformer of minimum energy value for each of the four families (called

**Table 3. Characteristics of the main set of conformations obtained for acyl-enzyme structures**

Number	Acyl-enzyme I	Acyl-enzyme II
Analyzed conformers	1 916	1 413
Families	202	197
Families with more than 16 members	13	12
(% of total conformers)	(80)	(70)
Largest families	4	4
(% of total conformers)	(70)	(51)

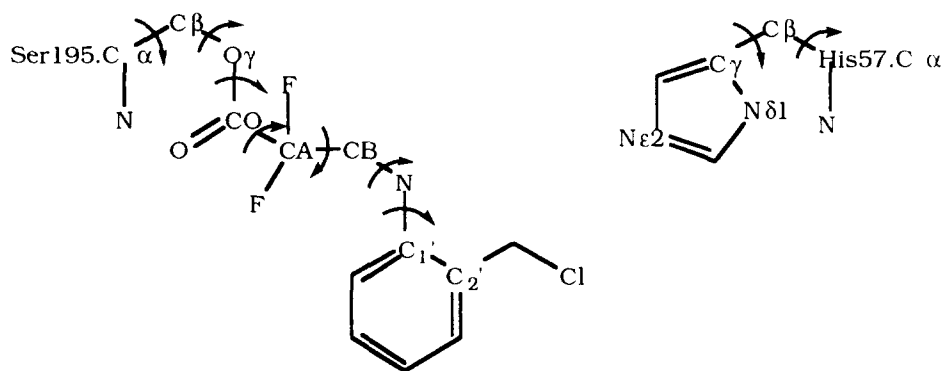
AE1 to AE4). These four resulting lowest energy conformations were extracted and minimized after replacing the dummy atom of the phenyl group by the chloromethyl group with orientation of the chlorine atom opposite to that of the His57.Nε2 (c', Figure 1). A distance range constraint was applied between the chloromethyl carbon of AA 231-1 (C7') and the nitrogen His57.Nε2. The characteristics of the four minimized structures AE1–AE4 are summarized in Table 4. In all cases, the side chain of Ser195 had a similar conformation [ $-77 < \chi_1 (^{\circ}) < -47$ ]. Owing to the values of the torsion angles  $\chi_1$  and  $\chi_2$ , the His57 position was found in the "out" position ( $170 < \chi_1 (^{\circ}) < 173$  and  $31 < \chi_2 (^{\circ}) < 67$ ). The donor (His57.Nδ1)–acceptor (Asp102.Oδ1) distance (6 Å) was not compatible with the formation of the hydrogen bonds found when His57 is in the "in" position (Color Plate 2). Comparison between the different torsion angle values of the "opened" inhibitor linked to the Ser195.Oγ atom showed that the flexibility of this compound was not impeded. By the positions of the side chain of His57 and of the phenyl ring of AA 231-1 for subsequent

alkylation, two groups were distinguished: group I with AE1 and AE2, and group II with AE3 and AE4 (Color Plate 2). The energy of these structures was approximately  $-270 \text{ kcal mol}^{-1}$ .

### Inactivated enzyme

The four final structures obtained for the acyl–enzyme complex were modified to build the inactivated enzyme. A bond was created between the His57.Nε2 and AA 231-1.C7' atoms and the atom types of the His57 imidazole ring were modified (deprotonation of His57.Nδ1 was needed). Optimization was then performed without constraint. The His57 position in the *bis*-adduct complex was not affected by minimization in comparison with the corresponding acyl–enzyme complex: the  $\chi_1$  and  $\chi_2$  torsion angles shifts were smaller than  $7^{\circ}$  (Figure 8). These final structures displayed an energy of  $-270 \text{ kcal mol}^{-1}$ .

**Table 4. Representative conformers of the acyl–enzyme complex formed between AA 231-1 and HLE, and obtained after minimization**



Family	AE1	AE2	AE3	AE4
$\chi_1$ angle of Ser195 ( $^{\circ}$ )				
N-Cα-Cβ-Oγ	-53	-47	-77	-58
Angle ( $^{\circ}$ )				
Cα-Cβ-Oγ-CO	96	-178	82	83
Angle ( $^{\circ}$ )				
Cβ-Oγ-CO-CA	169	-139	167	115
Angle ( $^{\circ}$ )				
Oγ-CO-CA-CB	-67	102	-74	55
Angle ( $^{\circ}$ )				
CO-CA-CB-N	-127	173	-133	162
Angle ( $^{\circ}$ )				
CA-CB-N-C1'	100	-153	-130	167
Angle ( $^{\circ}$ )				
CB-N-C1'-C2'	126	107	-95	-128
$\chi_1$ angle of His57 ( $^{\circ}$ )				
N-Cα-Cβ-Cγ	170	171	171	173
$\chi_2$ angle of His57 ( $^{\circ}$ )				
Cα-Cβ-Cγ-Nδ1	31	32	67	63
Distance (Å) C7'-Nε2	2.6	2.6	2.6	2.6
Energy ( $\text{kcal mol}^{-1}$ )	-269.2	-272.4	-268.5	-261.9

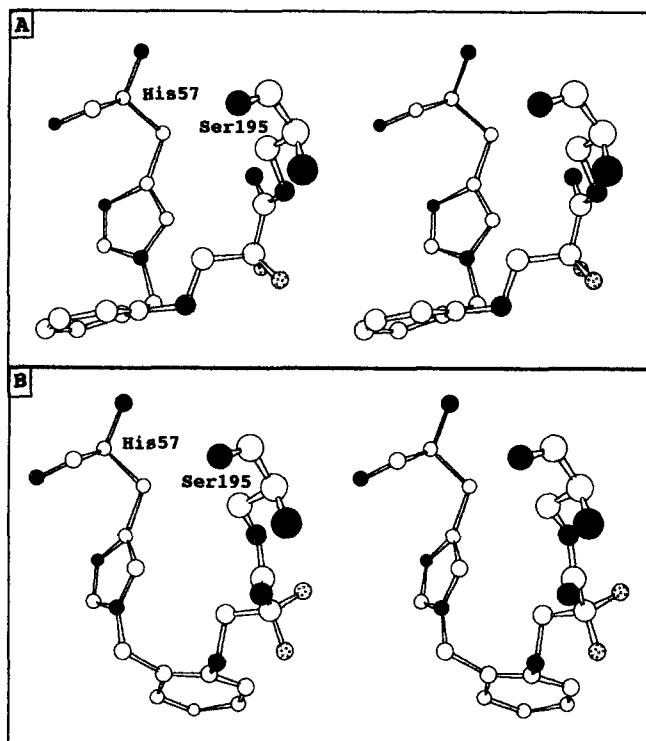


Figure 8. Stereoview of the two lowest energy minimized structures of inactivated enzyme deriving from AE2 (A) and AE3 (B) acyl-enzyme structures. Hydrogen atoms are not shown. See Figure 6 for symbols.

## DISCUSSION

The structural characteristics of the conformers of AA 231-1 are very similar to the crystalline structure of 1-(2-bromophenyl) azetidin-2-one: no pyramidality of the nitrogen atom and an amide bond length C2-N1 (1.32 Å) slightly shorter than the normal amide bond length (1.35 Å). This is also consistent with data obtained from crystal structures and microwave spectroscopy previously reported for related mono- $\beta$ -lactams.<sup>24-26</sup> In bicyclic  $\beta$ -lactam compounds such as tazobactam<sup>27</sup> or a carbapenam derivative,<sup>28</sup> the corresponding atom was pyramidal (sum of the angles around the nitrogen amide significantly less than 360°). It should be emphasized that different results were obtained depending on the atom types and force fields used in molecular mechanics. For examples, previous molecular mechanics studies on 1-(2-bromophenyl) azetidin-2-one structure with MM2 force field gave similar results whereas Amber force field calculations led to a significant pyramidality of the nitrogen.<sup>29</sup> Using Tripos force field and the N.amide atom type for nitrogen, the modeled configuration of the inhibitor is in agreement with the crystallographic data of related compounds. Unlike 1-(2-bromophenyl) azetidin-2-one taken as reference, the two rings of AA 231-1 are not found to be coplanar. This absence of coplanarity between the  $\beta$ -lactam and the phenyl cycles is due to steric hindrance of the chloromethyl group [compared with a unique bromine atom in 1-(2-bromophenyl)-azetidin-2-one] with AA 231-1.O5 atom (RB1  $\sim 0^\circ$ ) or with the hydrogen atoms bound to AA 231-1.C4 (RB1  $\sim 180^\circ$ ).

The reversible binding of AA 231-1 in the active site of HLE may occur with the localization of its carbonyl oxygen atom in the oxyanion hole and a favorable orientation for the formation of a tetrahedral intermediate. It was also found in a complex of HLE with a protein inhibitor studied by X-ray crystallography.<sup>11</sup> The  $\beta$ -lactam ring is located in the S<sub>1</sub> subsite similarly to the alanyl or valyl residue at the P<sub>1</sub> position of peptidic ligands. The *gem*-difluoro group, which enhances the electrophilicity of the carbonyl carbon, is in close contact with the S<sub>1</sub> subsite amino acids (Phe192 and Val216). Its size does not prevent the attack by the active serine. The  $\beta$ -lactam ring position allows the attack by the Ser195.O $\gamma$  atom on the  $\alpha$  face. A similar result was reported with the molecular modeling of monocyclic and bicyclic  $\beta$ -lactams acting as HLE inactivators.<sup>30-33</sup> The conformations of AA 231-1 in the Michaelis complex are different from those of the inhibitor alone ( $-157$  or  $134^\circ$  for the RB1 angle instead of  $-60$  or  $60^\circ$ ). The Phe192 residue of HLE may stabilize the Michaelis complex<sup>30</sup> by hydrophobic interactions as its phenyl ring forms an edge-to-face contact with that of AA 231-1. This type of aromatic-aromatic interaction is defined by an angle between the two phenyl rings in the range  $30$ – $90^\circ$  and a distance between the centroids of these two cycles in the range  $4.5$ – $7.0$  Å.<sup>34</sup> Such stabilization of the ligand-enzyme complex by an aromatic-aromatic interaction was found in several cases (a 6-benzyl-3-chloropyrone/ $\alpha$ -chymotrypsin<sup>35</sup>; a benzyl-substituted phosphonate inhibitor/ $\beta$ -lactamase<sup>36</sup>).

This modeling study allows us to propose a site of alkylation of HLE by AA 231-1. A histidine was alkylated as shown by an amino acid analysis of PPE inactivated by AA 231-1, which revealed the loss of one of six histidine residues.<sup>37</sup> Within a sphere of 8.5 Å radius centered on Ser195.C $\beta$ , only two histidine residues are found: His40 or His57, the latter being the most accessible residue. This radius was estimated by addition of the largest distance between Ser195.C $\beta$  and AA 231-1.C7' (theoretical extended conformation of the "opened" inhibitor), to a distance of 2 Å for the approach of AA 231-1.C7' by a nucleophilic atom. The mechanism of alkylation with an atom of the imidazole ring of a histidine residue may involve either a direct S<sub>N</sub>2 nucleophilic displacement or a methylene quinoniminium intermediate. In both cases, the same conditions of attack are required. Choosing the Ne2 atom, which is frequently involved in such processes,<sup>12,13,38,39</sup> the conformational analysis of the acyl-enzyme excludes alkylation of His40 by AA 231-1. Thus, His57 appears as the unique site of alkylation. It is found that the "out" position is necessary for alkylation. A covalent *bis*-adduct with HLE may be easily formed without large changes (acyl-enzyme compared to inactivated enzyme). This type of covalent enzyme-inhibitor complex has been found for the crystal structures of PPE with 7-amino-3-(2-bromoethoxy)-4-chloroisocoumarin<sup>38</sup> or a cephalosporin (i.e., a bicyclic  $\beta$ -lactam),<sup>39</sup> and of HLE with two peptide chloromethyl ketones.<sup>12,13</sup> In these structures, His57 is in the "in" position except for the complex between PPE and the cephalosporin. Such variations in the His57 position are also observed for stable acyl-enzyme complexes with PPE: "in" position for two peptidic<sup>40,41</sup> and one heterocyclic<sup>42</sup> inhibitors; "out" position for three other heterocyclic inhibitors.<sup>43,44</sup> Conse-

quently, a systematic rule cannot be established for the His57 position in enzyme-inhibitor complexes.

## CONCLUSION

Systematic searches and molecular mechanics have been used to propose a model for AA 231-1, a suicide substrate of HLE and for the different stages of the mechanism of inhibition of HLE. We studied the whole enzyme structure with modifications of the method developed by Naruto *et al.*<sup>45</sup> Their method dealt with the interaction of a haloenol lactone suicide substrate with a construction of the active site of  $\alpha$ -chymotrypsin. Our use of the complete enzyme structure appears more accurate with respect to all permissible intermolecular vdW contacts between enzyme and inhibitor. It also prevents deformations of the active site model during minimization calculations that would be incompatible with the whole enzyme structure. Crystallographic studies and molecular dynamic simulations of the interaction of inhibitors or substrates with PPE demonstrated that elastases act via a "lock-and-key" mechanism with limited mobility of His57 and Ser195 residues.<sup>1,46-48</sup> Rotation of these two side chains seems sufficient to examine the binding mode of the inhibitor. Such molecular mechanics studies are useful when crystal structures of HLE or PPE complexed with inhibitors are unavailable. In addition, no structural information on the complexes formed prior to the inactivated enzyme can be obtained from crystallographic data. This work, supported by biochemical studies, agrees with the hypothesis of alkylation of His57 residue by AA 231-1 leading to the inactivated enzyme. The aim of our molecular modeling studies was to develop a strategy for the study of the interaction of an *N*-aryl azetidinone with HLE. Its application to other  $\beta$ -lactams inactivator structures will be useful in predicting new and potentially more active inhibitors of HLE.

## ACKNOWLEDGMENTS

Dr. J.-P. Mornon is warmly acknowledged for carefully reading the manuscript and making fruitful suggestions. We thank ANVAR and ADIR for their financial support and the Ministère de l'Enseignement Supérieur et de la Recherche for a fellowship (I.V.).

## REFERENCES

- 1 Bode, W., Meyer, E., and Powers, J.C. Human leukocyte and porcine pancreatic elastase: X-ray structures, mechanism, substrate specificity and mechanism-based inhibitors. *Biochemistry* 1989, **28**, 1951-1963
- 2 Ménard, R. and Storer, A.C. Oxyanion hole interactions in serine and cysteine proteases. *Biol. Chem. Hoppe-Seyler* 1992, **373**, 393-400
- 3 Snider, G.L. Protease-antiprotease imbalance in the pathogenesis of emphysema and chronic bronchial injury: A potential target for drug development. *Drug Dev. Res.* 1987, **10**, 235-253
- 4 Robert, L. and Hornebeck, W. *Elastases and Elastin*, Vol. II. CRC Press, Boca Raton, Florida, 1989
- 5 Edwards, P.D., and Bernstein, P.R. Synthetic inhibitors of elastase. *Med. Res. Rev.* 1994, **14**, 127-194
- 6 Wakselman, M., Joyeau, R., Kobaiter, R., Boggetto, N., Vergely, I., Maillard, J., Okochi, V., Montagne, J.-J., and Reboud-Ravaux, M. Functionalized *N*-aryl azetidinone as novel mechanism-based inhibitors of neutrophil elastase. *FEBS Lett.* 1991, **282**, 377-381
- 7 Maillard, J.-L., Favreau, C., Reboud-Ravaux, M., Kobaiter, R., Joyeau, R., and Wakselman, M. Biological evaluation of the inhibition of neutrophil elastase by a synthetic  $\beta$ -lactam derivative. *Eur. J. Cell. Biol.* 1990, **52**, 213-218
- 8 Reboud-Ravaux, M., Vergely, I., Maillard, J., Favreau, C., Kobaiter, R., Joyeau, R., and Wakselman, M. Prevention of some types of inflammatory damage using AA 231-1, a fluorinated  $\beta$ -lactam. *Drugs Exp. Clin. Res.* 1992, **5**, 159-162
- 9 Maillard, J.-L., Favreau, C., Vergely, I., Reboud-Ravaux, M., Joyeau, R., Kobaiter, R., and Wakselman, M. Protection of vascular basement membrane and microcirculation from elastase-induced damage with a fluorinated  $\beta$ -lactam derivative. *Clin. Chim. Acta* 1992, **213**, 75-86
- 10 Williams, H.R., Lin, T.-Y., Navia, M.A., Springer, J.P., McKeever, B.M., Hoogsteen, K., and Dorn, C.P., Jr. Crystallization of human neutrophil elastase. *J. Biol. Chem.* 1987, **262**, 17178-17181
- 11 Bode, W., Wei, A.-Z., Huber, R., Meyer, E., Travis, J., and Neumann, S. X-ray crystal structure of the complex of human leukocyte elastase (PMN elastase) and the third domain of the turkey ovomucoid inhibitor. *EMBO J.* 1986, **5**, 2453-2458
- 12 An-Zhi, W., Mayr, I., and Bode, W. The refined 2.3 Å crystal structure of human leukocyte elastase in a complex with a valine chloromethyl ketone inhibitor. *FEBS Lett.* 1988, **234**, 367-373
- 13 Navia, M.A., McKeever, B.M., Springer, J.P., Lin, T.-Y., Williams, H.R., Fluder, E.M., Dorn, C.P., and Hoogsteen, K. Structure of human neutrophil elastase in complex with a peptide chloromethyl ketone inhibitor at 1.84 Å resolution. *Proc. Natl. Acad. Sci. U.S.A.* 1989, **86**, 7-11
- 14 SYBYL molecular modeling software, Tripos Associates, St. Louis, Missouri (1989)
- 15 Clarck, M., Cramer, R.D., III, and van Opdenbosch, J. Validation of the general purpose Tripos 5.2 force field. *J. Comput. Chem.* 1989, **10**, 982-1012
- 16 Fujiwara, H., Varley, R.L., and van der Veen, J.M. Conformation of 1-(2-bromophenyl) azetidin-2-one and 1-(2-bromophenyl) pyrrolidin-2-one. *J. Chem. Soc. Perkin Trans. II* 1977, 547-550
- 17 Bernstein, F.C., Koetzel, T.F., Williams, G.J.G., Meyer, E.F., Brice, M.D., Rodgers, J.R., Kennard, O., Shimanouchi, T., and Tasumi, M. The protein data bank: A computer-based archival file for macromolecular structures. *J. Mol. Biol.* 1977, **112**, 535-542
- 18 Meyer, E., Cole, G., and Radhakrishnan, R. Structure of native porcine pancreatic elastase at 1.65 Å resolution. *Acta Crystallogr.* 1988, **B44**, 26-38
- 19 Bürgi, H.B., Dunitz, J.D., Lehn, J.M., and Wipff, G. Stereochemistry of reaction paths at carbonyl centres. *Tetrahedron* 1974, **30**, 1563-1572



- 20 Schechter, I. and Berger, A. On the size of the active site in proteases. I. Papain. *Biochem. Biophys. Res. Commun.* 1967, **27**, 157–162
- 21 Anderson, M.W., Begley, M.J., and Jones, R.C.F. Dihydroimidazoles in synthesis: C-Acylation of lithiodihydroimidazoles. *J. Chem. Soc. Perkin Trans. I* 1984, 2599–2602
- 22 Bonnett, R., Hursthouse, M.B., North, S.A., and Trotter, J. On the aromaticity of isoindole. X-ray analysis of 2-benzylisoindole. *J. Chem. Soc. Perkin Trans. II* 1985, 293–296
- 23 Gao, J. and Xia, X. A two-dimensional energy surface for a type II  $S_N2$  reaction in aqueous solution. *J. Am. Chem. Soc.* 1993, **115**, 9667–9675
- 24 Chambers, R. and Doedens, R. 3-Chloro-3-cyano-1-cyclohexyl-4-(phenylthio)-2-azetidinone. A substituted monocyclic  $\beta$ -lactam. *Acta Crystallogr.* 1980, **B36**, 1507–1510
- 25 Lee, Y.H., Cho, S.-I., Kim, E., Shin, H.-S., Ruble, J.R., and Craven, B.M. L-1-Benzyl-4-mesomethyl-2-azetidinone. *Acta Crystallogr.* 1990, **C46**, 120–122
- 26 Marstokk, K.-M., Møllendal, H., Samdal, S., and Ungerud, E. The structure of gaseous 2-azetidinone as studied by microwave spectroscopy, electron diffraction and *ab initio* calculations. *Acta Chem. Scand.* 1989, **43**, 351–363
- 27 Toomer, C.A., Schwalbe, C.H., Ringan, N.S., Lambert, P.A., Lowe, P.R., and Lee, V.J. Structural studies on tazobactam. *J. Med. Chem.* 1991, **34**, 1944–1947
- 28 Désilets, D., Bélanger-Gariépy, F., Hanessian, S., and Brisse, F. Structure and stereochemistry of a carbapenam derivative. *Acta Crystallogr.* 1987, **C43**, 919–922
- 29 Chung, S.K. and Chodosh, D.F. Computer graphics/molecular mechanics studies of  $\beta$ -lactam antibiotics. Geometry comparison with X-ray crystal structures. *Bull. Korean Chem. Soc.* 1989, **10**, 185–190
- 30 Knight, W.B., Green, B.G., Chabin, R.M., Gale, P., Maycock, A.L., Weston, H., Kuo, D.W., Westler, W.M., Dorn, C.P., Finke, P.E., Hagmann, W.K., Hale, J.J., Liesch, J., MacCoss, M., Navia, M.A., Shah, S.K., Underwood, D., and Doherty, J.B. Specificity, stability, and potency of monocyclic  $\beta$ -lactam inhibitors of human leukocyte elastase. *Biochemistry* 1992, **31**, 8160–8170
- 31 Shah, S.K., Dorn, C.P., Jr., Finke, P.E., Hale, J.J., Hagmann, W.K., Brause, K.A., Chandler, G.O., Kissinger, A.L., Ashe, B.M., Weston, H., Knight, W.B., Maycock, A.L., Dellea, P.S., Fletcher, D.S., Hand, K.M., Mumford, R.A., Underwood, D.J., and Doherty, J.B. Orally active  $\beta$ -lactam inhibitors of human leukocyte elastase-1. Activity of 3,3-diethyl-2-azetidinones. *J. Med. Chem.* 1992, **35**, 3745–3754
- 32 Doherty, J.B., Ashe, B.M., Barker, P.L., Blacklock, T.J., Butcher, J.W., Chandler, G.O., Dahlgren, M.E., Davies, P., Dorn, C.P., Jr., Finke, P.E., Firestone, R.A., Hagmann, W.K., Halgren, T., Knight, W.B., Maycock, A.L., Navia, M.A., O'Grady, L., Pisano, J.M., Shah, S.K., Thompson, K.R., Weston, H., and Zimmerman, M. Inhibition of human leukocyte elastase. 1. Inhibition by C-7-substituted cephalosporin *tert*-butyl esters. *J. Med. Chem.* 1990, **33**, 2513–2521
- 33 Finke, P.E., Ashe, B.M., Knight, W.B., Maycock, A.L., Navia, M.A., Shah, S.K., Thompson, K.R., Underwood, D.J., Weston, H., Zimmerman, M., and Doherty, J.B. Inhibition of human leukocyte elastase. 2. Inhibition by substituted cephalosporin esters and amides. *J. Med. Chem.* 1990, **33**, 2522–2528
- 34 Burley, S.K. and Petsko, G.A. Aromatic-aromatic interactions: A mechanism of protein structure stabilization. *Science* 1985, **229**, 23–28
- 35 Ringe, D.B., Seaton, D.B., Gelb, M., and Abeles, R.H. Inactivation of chymotrypsin by 5-benzyl-6-chloro-2-pyrone:  $^{13}\text{C}$  NMR and X-ray diffraction analyses of the inactivator–enzyme complex. *Biochemistry* 1985, **24**, 64–68
- 36 Chen, C.C.H., Rahil, J., Pratt, R.F., and Herzberg, O. Structure of a phosphonate-inhibited  $\beta$ -lactamase: An analog of the tetrahedral transition state/intermediate of  $\beta$ -lactam hydrolysis. *J. Mol. Biol.* 1993, **234**, 165–178
- 37 Vergely, I. Ph.D. thesis. Université Denis Diderot (Paris 7), Paris, France, 1994
- 38 Vijayalakshmi, J., Meyer, E.F., Jr., Kam, C.-M., and Powers, J.C. Structural study of porcine pancreatic elastase complexed with 7-amino-3-(2-bromoethoxy)-4-chloroisocoumarin as a nonreactivable doubly covalent enzyme–inhibitor complex. *Biochemistry* 1991, **30**, 2175–2183
- 39 Navia, M.A., Springer, J.P., Lin, T.-Y., Williams, H.R., Firestone, R.A., Pisano, J.M., Doherty, J.B., Finke, P.E., and Hoogsteen, K. Crystallographic study of a  $\beta$ -lactam inhibitor complex with elastase at 1.84 Å resolution. *Nature (London)* 1987, **327**, 79–82
- 40 Takahashi, L.H., Radhakrishnan, R., Rosenfield, R.E., Jr., Meyer, E.F., Jr., Trainor, D.A., and Stein, M. X-ray diffraction analysis of the inhibition of porcine pancreatic elastase by a peptidyl trifluoromethylketone. *J. Mol. Biol.* 1988, **201**, 423–428
- 41 Takahashi, L.H., Radhakrishnan, R., Rosenfield, R.E., Jr., Meyer, E.F., Jr., and Trainor, D.A. Crystal structure of the covalent complex formed by a peptidyl  $\alpha,\alpha$ -difluoro- $\beta$ -keto amide with porcine pancreatic elastase at 1.78 Å resolution. *J. Am. Chem. Soc.* 1989, **111**, 3368–3374
- 42 Hernandez, M.A., Powers, J.C., Glinski, J., Oleksyszyn, J., Vijayalakshmi, J., and Meyer, E.F., Jr. Effect of the 7-amino substituent on the inhibitory potency of mechanism-based isocoumarin inhibitors for porcine pancreatic and human neutrophil elastases: A 1.85 Å X-ray structure of the complex between porcine pancreatic elastase and 7-[(*N*-tosylphenylalanyl)amino]-4-chloro-3-methoxyisocoumarin. *J. Med. Chem.* 1992, **35**, 1121–1129
- 43 Radhakrishnan, R., Presta, L.G., Meyer, E.F., Jr., and Wildonger, R. Crystal structures of the complex of porcine pancreatic elastase with two valine-derived benzoxazinone inhibitors. *J. Mol. Biol.* 1987, **198**, 417–424
- 44 Powers, J.C., Oleksyszyn, J., Narasimhan, L., and Kam, C.-M. Reaction of porcine pancreatic elastase with 7-substituted 3-alkoxy-4-chloroisocoumarins: Design of potent inhibitors using the crystal structure of the complex formed with 4-chloro-3-ethoxy-7-guanidinoisocoumarin. *Biochemistry* 1990, **29**, 3108–3118

- 45 Naruto, S., Motoc, I., Marshall, G.R., Daniels, S.B., Sofia, M.J., and Katzenellenbogen, J.A. Analysis of the interaction of haloenol lactone suicide substrates with  $\alpha$ -chymotrypsin using computer graphics and molecular mechanics. *J. Am. Chem. Soc.* 1985, **107**, 5262–5270
- 46 Lesyng, B. and Meyer, E.F., Jr. Thermodynamic cycle-perturbation study of the binding of trifluoroacetyl dipeptide anilide inhibitors with porcine pancreatic elastase. *Biopolymers* 1990, **30**, 773–780
- 47 Geller, M., Carlson-Golab, G., Lesyng, B., Swanson, S., and Meyer, E.F., Jr. Dynamical properties of the first enzymatic reaction steps of porcine pancreatic elastase. How rigid is the active site of the native enzyme? Molecular mechanics simulation. *Biopolymers* 1990, **30**, 781–796
- 48 Geller, M., Swanson, S.M., and Meyer, E.F., Jr. Simulations of dynamical properties of a Michaelis complex: Porcine pancreatic elastase and a hexapeptide, Thr-Pro-nVal-Leu-Tyr-Thr. *J. Biomol. Struct. Dynamics* 1990, **7**, 1043–1052